

Detection of Sub-Millimeter Surface Cracks using Complementary Split-Ring Resonator

by

Ali Albishi

A thesis
presented to the University of Waterloo
in fulfillment of the
thesis requirement for the degree of
Master of Applied Science
in
Electrical and Computer Engineering

Waterloo, Ontario, Canada, 2012

© Ali Albishi 2012

I hereby declare that I am the sole author of this thesis. This is a true copy of the thesis, including any required final revisions, as accepted by my examiners.

I understand that my thesis may be made electronically available to the public.

Abstract

Many interesting ideas have emerged from research on electromagnetic field interactions with different materials. Analyzing such interactions has extracted some essential properties of the materials. For example, extracting constitutive parameters such as permittivity, permeability, and conductivity, clarifies a material's behavior. In general, the electromagnetic field interacts with materials either in the far-field or near-field of a source. This study focuses on the principle of near-field microwave microscopy for detection purposes.

Many studies have focused on the use of an electrically small resonator, such as a split-ring resonator (SRR) and a complementary split-ring resonator (CSRR), to act as a near-field sensor for material characterization and detection. At the resonance frequency, the electric and magnetic energy densities are enhanced dramatically at certain locations in the resonator. Any disturbance of the field around such a resonator with a material under test causes the resonance frequencies to exhibit a shift that is used as an indicator of the sensor sensitivity. In this thesis, a single CSRR is used as a sensing element for detecting cracks in metal surfaces.

Many microwave techniques have been developed for crack detection. However, these techniques have at least one of the following drawbacks: working at high frequencies, measurement setup complexity and cost, and low sensitivity. The first part of this thesis presents a new sensor based on the complementary split-ring resonator (CSRR) that is used to detect sub-millimeter surface cracks. The sensing mechanism is based on perturbing the electromagnetic field around an electrically small resonator, thus initiating a shift in the resonance frequency. Investigation of the current distribution on a CSRR at the resonance frequency shows the critical location at which the enhanced energy is concentrated. In addition, the current distribution demonstrates the sensing element in the CSRR. The sensor is simple to fabricate and inexpensive, as it is etched-out in the ground plane of a microstrip-line using printed circuit board technology. The microstrip-line excites the CSRR by producing an electric field perpendicular to the surface of the CSRR. The sensor exhibits a frequency shift of more than 240 MHz for a 200 μm crack.

In the second part of this thesis, the sensitivity of the sensor is increased by filling the same crack with a dielectric material such as silicon oil. While using CSRR to scan a block with 200 μm wide and 2 mm depth dielectric filled crack, the resonance frequency of the sensor shifts 435 MHz more than a case scanning a solid aluminum. Finally, the total Inductance of a CSRR for miniaturizing purposes is increased using either lumped or distributed elements. In this thesis, the designs and the results are validated experimentally and numerically.

Acknowledgements

All praises are due to Allah for giving me the ability to write this work. All praises are due to Allah for giving me the honor of helping the humanity by contributing to enrich its knowledge.

I would like to express my deepest gratitude to my advisor Professor Omar M. Ramahi. I cannot thank him enough for his thoughtful guidance, generous supports, and friendly discussions which helped me to improve my academic knowledge. I believe that having discussion with him is a peerless privilege.

I am also grateful to my committee members, Professor Raafat R. Mansour and Professor Safieddin Safavi-Naeini for serving in my examination committee and for their invaluable feedback.

Special thanks to Mohammed Said Boybay and Babak Alavikia for their support and assistance during my studies.

I would like to acknowledge my colleagues, Mohammed Said Boybay, Babak Alavikia, Hussein Attia, Mohammad Bait Suwailam, Zhao Ren, Na'el Suwan, Mohammad Alshareef, Abdulaziz Alqahtani, Thamer Almoneef, Ahmed Ashoor, and Miguel Ruphuy. Their friendly discussion always inspires new ideas.

I would like to thank Mazen Alsabaan and Essam Tobaishi for their help and assistance in settling in Canada.

I would like to thank my family for their support, patient, and for believing in me; my father (Mohammed) and my mother (Salihah), my brothers (Ayed, Abdullah, and Bandar) and my sisters (Shara, Kazma, Rana, Haya, Hoda, Maram).

Atha, my dear wife, is always my source of inspiration. I owe Atha my deepest gratitude for her infinite patience that accompanies me along this long journey to fulfil my goals. Atha and my twins (Mohammed and Abdulaziz) are my source of strength. Their love is my motivation, and their happiness is my ultimate goal.

This work was financially supported by King Saud University, Saudi Arabia.

Dedication

To my parents for their unconditional love and support,
To my beloved wife Atha who gave color to my life.

Table of Contents

| | |
|--|-------------|
| List of Figures | viii |
| 1 Introduction | 1 |
| 1.1 Motivation | 1 |
| 1.2 Background | 2 |
| 1.2.1 Near-Field Microwave Microscopy | 2 |
| 1.2.2 Microwave and Millimeter Wave Technology Techniques | 3 |
| 1.3 Thesis Contributions | 4 |
| 1.4 Thesis Organization | 4 |
| 2 Complementary Split-Ring Resonator Sensor | 6 |
| 2.1 Sensor Design | 6 |
| 2.2 Excitation Mechanism | 7 |
| 2.3 Current Distribution on CSRR at Resonance Frequency and Realization of Sensing Element | 9 |
| 3 Measurements | 12 |
| 3.1 Measurements procedure | 12 |
| 3.2 Result and Discussion | 12 |

| | | |
|----------|---|-----------|
| 4 | Sensitivity Enhancement of Crack Detection and Miniaturization of CSRR | 20 |
| 4.1 | Filling a Crack with a Dielectric Material | 20 |
| 4.2 | Increasing the Total Inductance of CSRR for Miniaturizing Purposes | 22 |
| 5 | Conclusion | 28 |
| 5.1 | Conclusion | 28 |
| | References | 29 |

List of Figures

| | | |
|-----|---|----|
| 1.1 | The CSRR printed on the ground plane of a microstrip line with its fabricated dimensions, $g = s = 0.16$ mm and $t = 0.27$ mm | 5 |
| 2.1 | A schematic showing the geometry of the sensor. The total size of the sensor is 3 mm. When a metallic plate is brought into close proximity with the sensor, changes occur in the capacitance and inductance between the center island and the ground plane. As a result, any irregularity on the surface of the plate is reflected in the resonance frequency. | 7 |
| 2.2 | The sensor is placed as a defect on the ground plane of a microstrip line. The microstrip line generates a perpendicular electric field on the ground plane to excite the CSRR. As the sample under test is placed below the ground plane of the microstrip line, the resonance frequency of the CSRR changes. | 8 |
| 2.3 | Minimum transmission of the sensor obtained from full-wave solver HFSS and measurement of the sensor in case without a crack | 9 |
| 2.4 | Simulated current distribution on a CSRR at the resonance frequency of around 6.95 GHz | 10 |
| 2.5 | Magnetic field lines around the narrow lines (A and B) as illustrated in Fig. 2.4 | 11 |
| 3.1 | A schematic showing the microstrip line fed CSRR sensor and the scanning procedure. | 13 |
| 3.2 | Current distribution on an aluminum plate for a crack with a width and depth of $100\mu\text{m}$ and 2mm, respectively. | 14 |
| 3.3 | The experimental setup. | 15 |

| | | |
|-----|--|----|
| 3.4 | The frequency of minimum transmission for both simulated and experimental results in the case of a crack with a width and depth of $100\mu\text{m}$ and 2 mm, respectively. | 16 |
| 3.5 | Minimum transmission of the sensor for a crack width (w) of $100\mu\text{m}$ compared with solid aluminium. For case 1, the crack depth (h) is 2 mm. For case 2, the crack depth (h) is 1 mm. | 17 |
| 3.6 | Minimum transmission of the sensor for a crack width (w) of $200\mu\text{m}$ compared with solid aluminium. For case 1, the crack depth (h) is 2 mm. For case 2, the crack depth (h) is 1 mm. | 18 |
| 3.7 | Shift in the minimum transmission frequency as a function of the position along a straight line that is perpendicular to the cracks. | 19 |
| 4.1 | Minimum transmission of the sensor for a crack width (w) of $200\mu\text{m}$ and depth of 2 mm: for case 1, a solid aluminum; case 2, the crack without silicon oil; case 3, the crack filled with silicon oil | 21 |
| 4.2 | Minimum transmission coefficient of the sensor obtained from the full-wave simulator HFSS and measurement of 6 mm CSRR for the case without a crack after adding the two inductors of value 20 nH. | 23 |
| 4.3 | Minimum transmission coefficient of the sensor obtained from measurement with and without inductors of 6 mm CSRR. | 24 |
| 4.4 | Simulated current distribution on a new design of CSRR sensor using spiral shape at the resonance frequency of around 3.781 GHz. | 25 |
| 4.5 | Minimum transmission coefficient of the two sensor obtained from the full-wave simulator HFSS at the resonance frequency of 3 mm CSRR. | 26 |
| 4.6 | Minimum transmission of the new design of CSRR sensor using spiral shape for crack width (w) of $100\mu\text{m}$ and the crack depth (h) is 2 mm compared with solid aluminium. | 27 |

Chapter 1

Introduction

1.1 Motivation

Inspection of metal surfaces for damage and failure is critical to accident prevention in many environments. The mechanical integrity of metal surfaces in a host of systems such as aircraft fuselages, nuclear power plant steam generator tubing, and steel bridges amongst others can be compromised by metal fatigue. Metal fatigue, which is caused by a material's cyclic loading, is a critical issue in structure failure and deterioration. Usually the fatigue process involves two different stages: initiation life and propagation life. The initiation life is the period during which a small crack starts to develop. The propagation life, which starts after the initiation life with no transition period between, is the total time taken for a crack to start growing and developing until a cracked structure fails [5]. Such fatigue can take the shape of sub-millimeter size cracks. Hence, surface detection, especially at the earliest stages, is one of the most important steps of metallic-surface inspection, maintenance and reliability. In addition, detection of such cracks, especially those concealed by paint, is a critical step in metallic-surface inspection. Several techniques have been developed to determine the extent of any fatigue. For non-destructive testing (NDT), ultrasound and eddy current techniques are the two conventional methods for crack detection. Although such techniques have high sensitivity and resolution, they cannot be applied in some situations [13]. For example, ultrasound techniques cannot detect sub-millimeter cracks close to the surface, especially those smaller than 5 mm. In such scenarios, other methods are preferred, such as eddy current [13]. The eddy current technique has certain drawbacks. For instance, an eddy current, which causes a magnetic field, is generated in a metal surface using a coil. If the metal surface has a defect, it will disturb the field, and measuring

the changes in the coil impedance will indicate the defect. [6]. However, in most cases this change is very weak. Thus, to address these limitations, microwave and millimeter wave technology techniques have emerged for crack detection.

1.2 Background

1.2.1 Near-Field Microwave Microscopy

Many interesting ideas have emerged from research on electromagnetic field interactions with different materials. Analyzing such interactions has extracted some essential properties of these materials. For example, extracting constitutive parameters such as permittivity, permeability, and conductivity clarifies a material's behavior. In general, the electromagnetic field interacts with materials either in the far-field or near-field of a source. For far-field interactions, the dimension of the material under test must be in the same order of magnitude of a wavelength of the radiation frequency, this limiting the use of far-field for imaging or detection purposes [3]. For example, the variation of materials changes on a scale much shorter than the wavelength of the source, so this particular technique requires the sample under test to be large, pure, and homogeneous. However, homogeneity of a material is not applicable for most samples, which instead are usually composites of more than one material [3]. Unlike far-field interactions, near-field interactions have a very high spatial resolution, so they overcome the problems found in property extractions of materials using far-field techniques.

Extensive research has studied the interactions between the field in near-zone of a source and materials under test. These studies have brought out very interesting techniques related to the principle of near-field microwave microscopy techniques for imaging and detection purposes [3]. in the near-field region of a source, the evanescent fields decay exponentially. The evanescent microwave technique involves using a probe with the size D that is much smaller than the wavelength of the excitation source [9]. The size discrepancy between probe and the wavelength of waves leads to some limitations. In electromagnetic field theory, the limitation created by extracting material properties smaller than one half the wavelength is referred to as the Abbe barrier. However, several studies have been reported to break this limit [7], [4].

In the evanescent microwave technique, the electromagnetic field is dramatically confined in region having a sub-wavelength dimensions. Thus, this technique can effectively extract material properties having smaller size than one half the wavelength [3]. Fundamentally, evanescent microwave probes must scan in close proximity to the materials

under test so that near-field waves are totally able to couple to the material. In the most measurements, the change in the resonance frequency and quality factor of an evanescent microwave probe is measured in the presence of material under test. In other words, the probe scans the material to extract its local properties and processes the results as images. In addition, the results indicate a changes in the material properties, so the results can be used for detection applications [3]. Moreover, many factors affect the total changes in the resonance frequency and the quality factor. The most important factors are the probe geometry, the distance between the probe and material, and the material properties.

Generally, electromagnetic waves penetrate into dielectric materials, and these penetrations depend on the materials properties. Thus, the use of evanescent waves for imaging and detection leads to many important applications in industries. In many situations, metal surfaces are painted with dielectric layers where the painting conceal any defect in the surfaces from visual inspection. For example, most aircraft fuselages are built from aluminum plates. The plates are concealed by special paint layers, so inspection of the metallic surface at the earliest stages is critical step in aircraft maintenance. Such a step will save life time and money. Consequently, researchers have extensively investigated several methods for crack detection in metallic surfaces. Among other techniques, microwave and millimeter wave technology techniques have brought many interesting solutions, especially for concealed and small cracks [24, 25, 26, 11, 23, 20, 16, 13, 14, 2, 19].

1.2.2 Microwave and Millimeter Wave Technology Techniques

Metallic-surface inspection for crack detection is very important step in metal surface maintenance; thus, many interesting ideas for crack detection have been proposed. In [24], the proposed technique is based on using an open-ended waveguide. When there is a crack on the surface of the metal, the near-field distribution at the end of the waveguide is perturbed, leading to a change in the reflection coefficient recorded using a diode detector. The sensor in [24] was able to detect a crack less than one millimeter wide; however, the operating frequency was around 20 GHz. Operating at high frequency increases the cost of the measurement equipment and setup. In addition, for sub-millimeter crack detection, the perturbation in the reflection coefficient is insignificant, which introduces detection difficulties. These difficulties have led to the use of highly accurate and reliable measurement equipment [13]. Although the open-ended waveguide sensor has been studied extensively to improve its performance by optimizing measurement parameters such as the position of the diode [25] and applied to different crack shapes [17], the sensing element of the system has remained the same. In [13], near-field microwave dual-behavior resonator (DBR) filters were proposed to detect micro-cracks in metal surfaces. In these filters, the shift

in the resonance frequency is observed and measured as an indicator of the presence of cracks. Two DBR filters were designed with different high-frequency (HF) stub widths of $W_{HF} = 100\mu\text{ m}$ and $W_{HF} = 50\mu\text{ m}$ for filter 1 and 2, respectively. The filters are tuned to operate at around 10 GHz, and the shift in the resonance frequency due to the presence of a micro-crack (Δf_r) is around 39 MHz for filter 1 and 51 MHz for filter 2. However, the operating frequency is high, and Δf_r is low, thus reducing its sensitivity. In addition, the minimum transmission and reflection coefficient do not occur over a very narrow band, thus finding the resonant frequency is difficult. In [19], an antenna is used as a sensor for crack detection and monitoring. A rectangular patch antenna is used for this purpose. This sensor mechanism is based on observing the shift in the resonance frequencies for two modes. The first mode operates at 6.1 and the second mode operates at 7.6 GHz. The sensitivity of the sensor is low ($\Delta f_r = 48.7\text{ MHz/mm}$). Indeed, each crack detection method presented in the literature has at least one of the following disadvantages, either it operates at high frequency, which increases the cost of the associated circuitry, or its sensitivity is too low for crack detection.

1.3 Thesis Contributions

This thesis presents a novel sensor for detecting sub-millimeter size cracks, based on a shift in the resonance frequency of a complementary split-ring resonator (CSRR) printed on the ground plane of a microstrip line (Fig 1.1). The effectiveness of the sensor is demonstrated experimentally. The advantages of the CSRR sensor compared to other microwave techniques for crack detection is lower operating frequency, higher sensitivity, and relatively very low fabrication cost using printed circuit board technology.

1.4 Thesis Organization

The organization of this thesis is as follows. Chapter 2 provides details of the sensor design and excitation mechanism. In section 2.1, the sensor design realization using a full-wave finite element solver and the final fabricated dimensions of the sensor are presented. Section 2.2 presents the method chosen to excite the CSRR, and section 2.3 describes sensing elements identified by simulating the current distribution. The measurement procedure for crack detection is presented in Chapter 3, followed by results and discussion. Chapter 4 discusses the ability of presented sensor to detect cracks having width smaller than $100\mu\text{m}$.

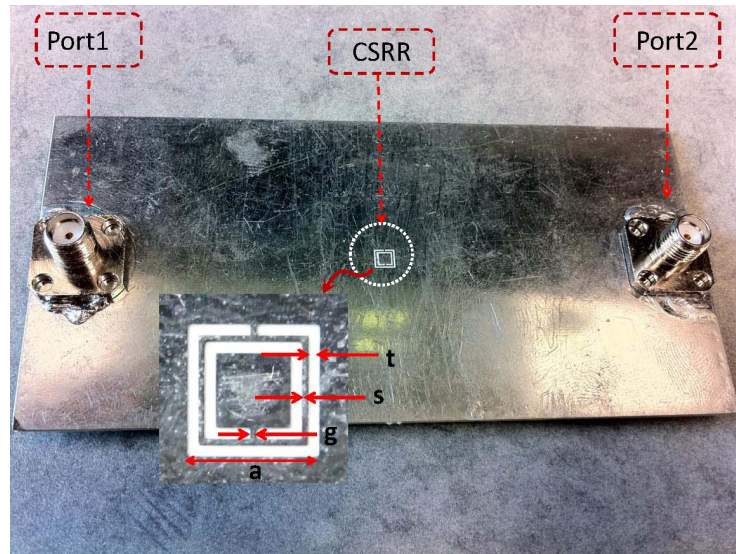


Figure 1.1: The CSRR printed on the ground plane of a microstrip line with its fabricated dimensions, $g = s = 0.16$ mm and $t = 0.27$ mm

Additionally, miniaturizing the CSRR sensor using lumped and distribution elements is shown in this chapter. Finally, Chapter 5 concludes the thesis.

Chapter 2

Complementary Split-Ring Resonator Sensor

2.1 Sensor Design

In the presented work, a single CSRR is used as a sensing element to detect sub-millimeter size cracks in metallic surfaces. The objective here is to design a sensor operating at around 7 GHz with the dimensions of $a = 3$ mm and $s = g = t = 0.2$ mm as shown in Fig. 2.1. This particular choice is based on the availability of relatively inexpensive microwave components. To achieve the design goals, one can use the approximate formula reported in [8], or more directly, use an eigenvalue solver to determine resonance frequency. In either approach, several design trials must be realized before a design is finalized that meets the frequency range criterion (resonance close to 7 GHz) in addition to having approximate size features that can be realized using a simple circuit board milling machine.

The CSRR structure has a planar shape with a center island connected to the surrounding ground planes by narrow lines as shown in Fig. 2.1. When there is a voltage difference between the center island and the surrounding ground plane, the current experiences a capacitance between the island and the ground plane and an inductance at the narrow lines that connects the two. Therefore, depending on the capacitance and the inductance, resonant behavior is observed. Typically, the larger the CSRR's dimensions, the lower its resonant frequency, as larger dimensions entail higher inductance and higher capacitance. As a result of the feature size of the fabrication technique, a CSRR that operates at around 7 GHz has been designed for this particular research. In order to minimize the overall size, the minimum feature size of 0.2 mm is used for the gap separation and the trace width of

the structure. Next, the eigenvalue solver of Ansys HFSS is used to find the overall size of the resonator to achieve the resonance within the frequency range of interest [1]. In order to detect a micro-crack, a 3 mm CSRR was designed, with a 1:8 mm square center island. The details of the design are presented in Fig. 2.1. However, due to fabrication limitations and milling machine tolerance, the final fabricated sensor had dimensions of $a = 3$ mm, $g = s = 0.16$ mm and $t = 0.27$ mm, as shown in Fig. 1.1. It must be emphasized, however, that the objective in designing the sensor is to achieve resonance frequency *close to* 7 GHz. Achieving resonance at a certain and precise frequency is of minor importance here.

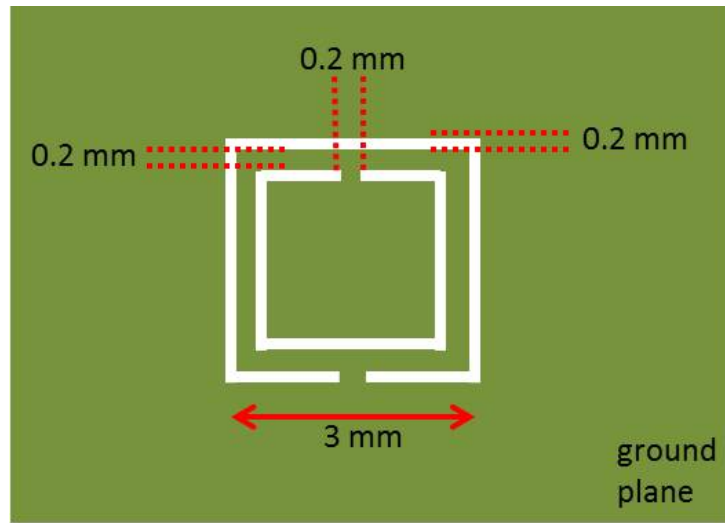


Figure 2.1: A schematic showing the geometry of the sensor. The total size of the sensor is 3 mm. When a metallic plate is brought into close proximity with the sensor, changes occur in the capacitance and inductance between the center island and the ground plane. As a result, any irregularity on the surface of the plate is reflected in the resonance frequency.

2.2 Excitation Mechanism

In order to excite the CSRR sensor, an electric field perpendicular to the surface of the sensor is needed and acts in a manner analogous to the much used split ring resonator structure. Therefore, a microstrip line structure was chosen for exciting the CSRR. The CSRR was etched out in the ground plan of the microstrip line. Previously, this structure was used as a stop band filter in [8]. Therefore, the microstrip line illuminated CSRR structure

exhibits stop band characteristics (a frequency range where the transmission coefficient becomes very small). The frequency at which the transmission coefficient is minimal depends on the resonance frequency of the CSRR. Therefore, when the material surface under test is placed underneath the CSRR, the material disturbs the electromagnetic field, leading to a change in the resonance frequency. A schematic of the sensor structure is shown in Fig. 2.2. The transmission coefficient is recorded using a Vector Network Analyzer (VNA). The microstrip line has been designed to match the internal impedance of the VNA in the measurement setup. It can be also designed to match the internal impedance of other possible feed circuitry. In order to have a characteristic impedance of 50Ω , the width of the microstrip line is selected to be 1.68 mm. A Rogers RO4350 substrate with a thickness of 0.75 mm, a permittivity of 3.66, and a loss tangent of 0.0031 was used for the fabrication. Figure 2.3 shows a strong agreement between the sensor behavior obtained from the simulation and the measurements.

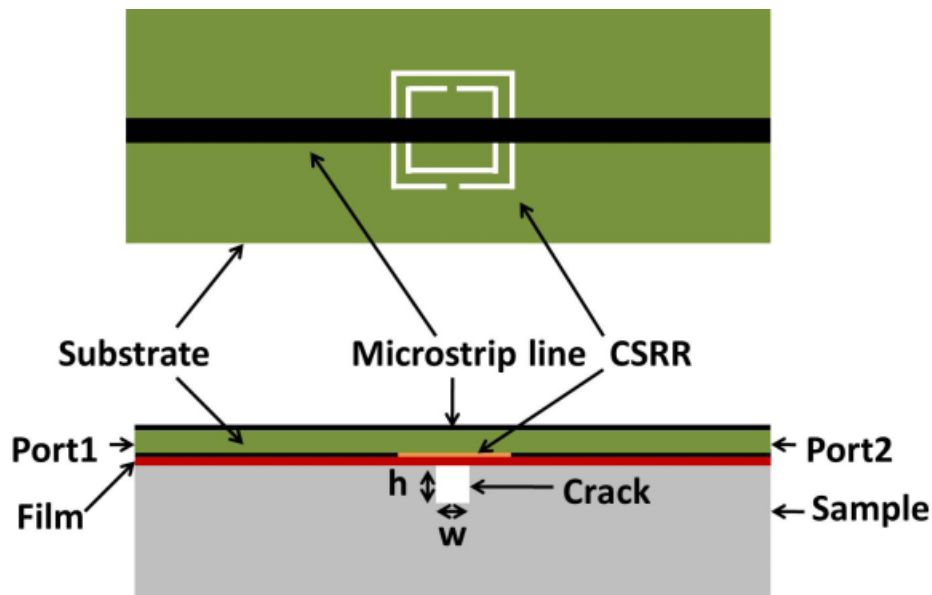


Figure 2.2: The sensor is placed as a defect on the ground plane of a microstrip line. The microstrip line generates a perpendicular electric field on the ground plane to excite the CSRR. As the sample under test is placed below the ground plane of the microstrip line, the resonance frequency of the CSRR changes.

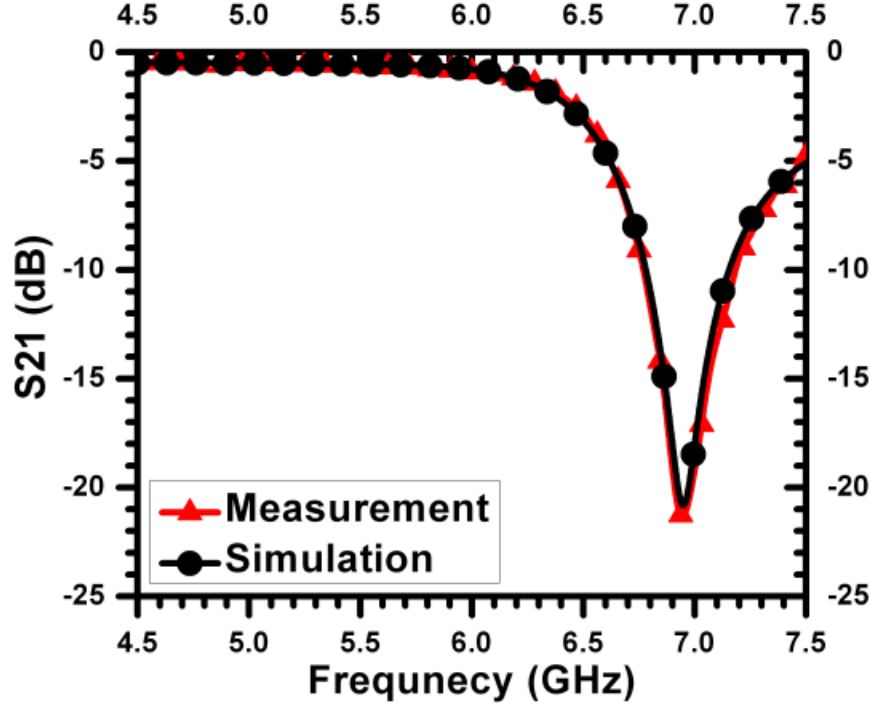


Figure 2.3: Minimum transmission of the sensor obtained from full-wave solver HFSS and measurement of the sensor in case without a crack

2.3 Current Distribution on CSRR at Resonance Frequency and Realization of Sensing Element

According to Pendry's work [21], resonance frequencies of a structure such as a CSRR, whose dimensions are much smaller than the wavelength of the radiation frequency, are due to the internal capacitance and inductance. At the resonance frequency, the electric and magnetic energy density is enhanced dramatically at a certain location in the structure. Investigation of such a location leads to critical applications such as sensing. In other words, by perturbing the electromagnetic field around a resonator, its resonance frequency exhibits a shift that depends on the material disturbing the field. Many studies have focused on the use of such resonators as sensing elements. For example, in [22], a split-ring resonator was used to resolve the dielectric properties of organic tissues. In addition, a biosensor device has been proposed based on a SRR. The sensor was used to recognize

DNA hybridization by observing a shift in the resonance frequency [15]. In this work, a single CSRR as a sensing element is used for detecting cracks in metal surfaces. For the purpose of studying a CSRR as a sensor for crack detection, one can study the behavior of the field around the resonator by showing the current distribution. Investigating the current distribution on the CSRR at the resonance frequency shows the critical location at which the enhanced energy is concentrated. The full-wave simulator HFSS was used to simulate the presented sensor excited by a microstrip line and plot the current distribution of the CSRR. Figure 2.4 demonstrates that, at resonance frequency, the narrow lines (A and B) have maximum current distribution on the CSRR. In addition, Figure 2.5 shows the maximum magnetic field observed at region A; obviously, region A is used as a sensing element in CSRR sensor, and is where the material under test will disturb the magnetic field. Hence, perturbing the magnetic field causes a shift in the resonance frequency.

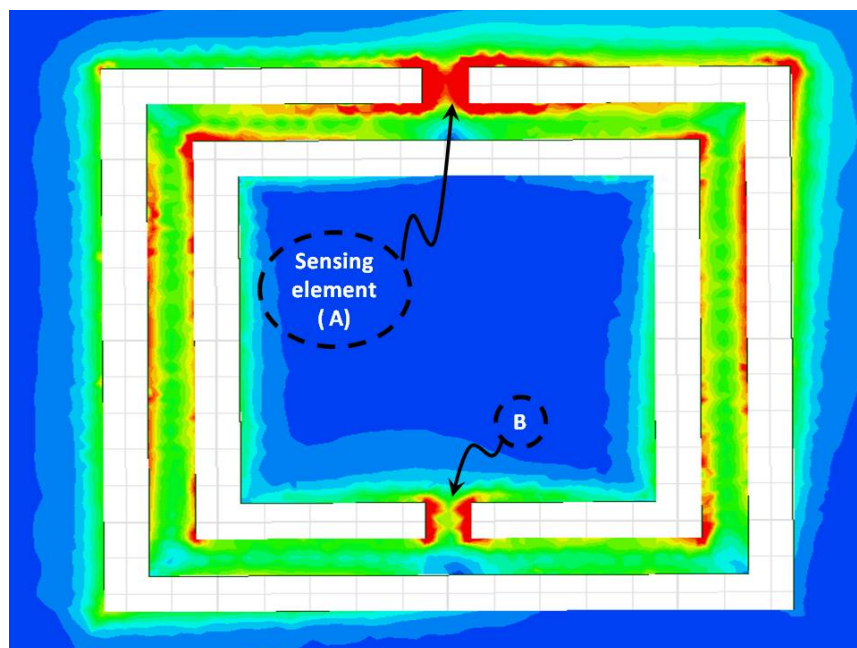


Figure 2.4: Simulated current distribution on a CSRR at the resonance frequency of around 6.95 GHz

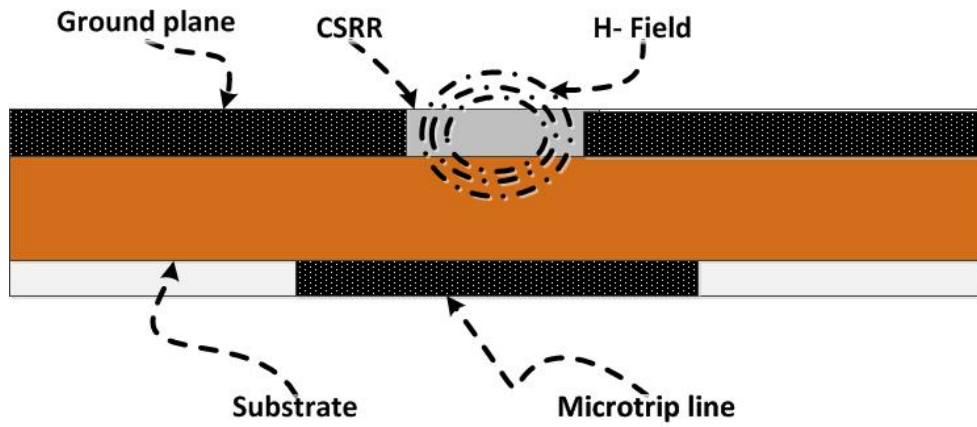


Figure 2.5: Magnetic field lines around the narrow lines (A and B) as illustrated in Fig. 2.4

Chapter 3

Measurements

3.1 Measurements procedure

Using microwave techniques for metal detection offers some critical advantages. For example, the metal under test might be covered by a layer of a dielectric coating. In measurements, a thin teflon film with a thickness of 0.0762 mm is used to cover an aluminum plate surface and also mimics a layer of paint or a dielectric coating that can possibly conceal a crack from visual inspection. Once the CSRR is designed to operate in a frequency range of interest, the resonance frequency is then recorded for a reference case defined to correspond to when the sensor is placed directly above a solid aluminum plate devoid of any defects or cracks. The sensing or crack scanning is performed by passing the sensor above an aluminum metallic plate, as shown in Fig. 3.1. When a crack is encountered, a change in the resonance of the CSRR is registered. The sensitivity of the sensor is determined by its ability to detect a crack of specific dimensions and the change or shift in the resonance frequency from the reference case.

3.2 Result and Discussion

To validate the concept of using CSRR as a sensor for crack detection, the proposed sensor was simulated using the full-wave simulator HFSS. The results show that when the sensor is passed over a crack, the crack disturbs the magnetic field around the position (A) as shown in Fig. 2.4, and the resonance frequency exhibits a shift. The measurements to confirm the simulation result were carried out on an aluminum plate with a crack. Figure 3.4 shows

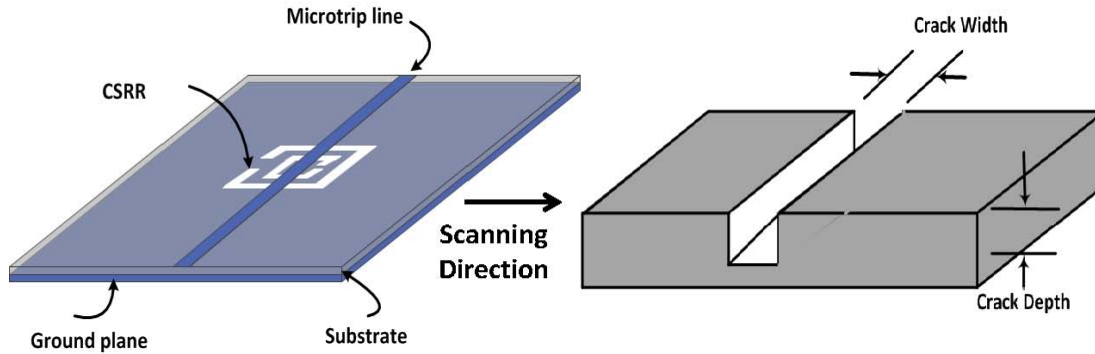


Figure 3.1: A schematic showing the microstrip line fed CSRR sensor and the scanning procedure.

the frequency of minimum transmission for both simulated and experimental results as the sensor is passed over a crack with a width and depth of $100\mu\text{m}$ and 1 mm , respectively. In addition, the current distribution on the aluminum plate at the resonance frequency when the crack passes region A is illustrated in Fig. 3.2. It shows, at the resonance frequency, a highly concentrated current on the surface of the cracked plate. As shown in Fig. 3.3, the measurement setup was utilized using an Agilent (45 MHz-50 GHz) vector network analyzer and two clips holding the sensor with an aluminum plate.

Figure 3.5 shows the frequency of minimum transmission when the sensor passes over a crack with a width and depth of $100\ \mu\text{m}$ and 1 mm , respectively. A shift of more than 240 MHz was realized with respect to the case without a crack. Figure 3.6 shows that a $200\ \mu\text{m}$ wide and 1 mm deep crack results in a frequency shift of more than 260 MHz , corresponding to an approximately 5% shift with respect to the case without a crack.

To test the ability of the sensor to discriminate between two closely spaced cracks, two parallel 0.1 mm wide cracks, 1 mm in depth is considered, separated by a distance of 1 mm . Next, the minimum transmission frequency is measured as the sensor was moved along a straight line perpendicular to the cracks. Figure 3.7 shows the shift in the minimum transmission frequency as a function of the position along the straight line. The first and second crack lines correspond to the 6 mm and 7 mm positions, respectively. Clearly, the proposed sensor is able to resolve two 0.1 mm cracks separated by a distance of only 1 mm .

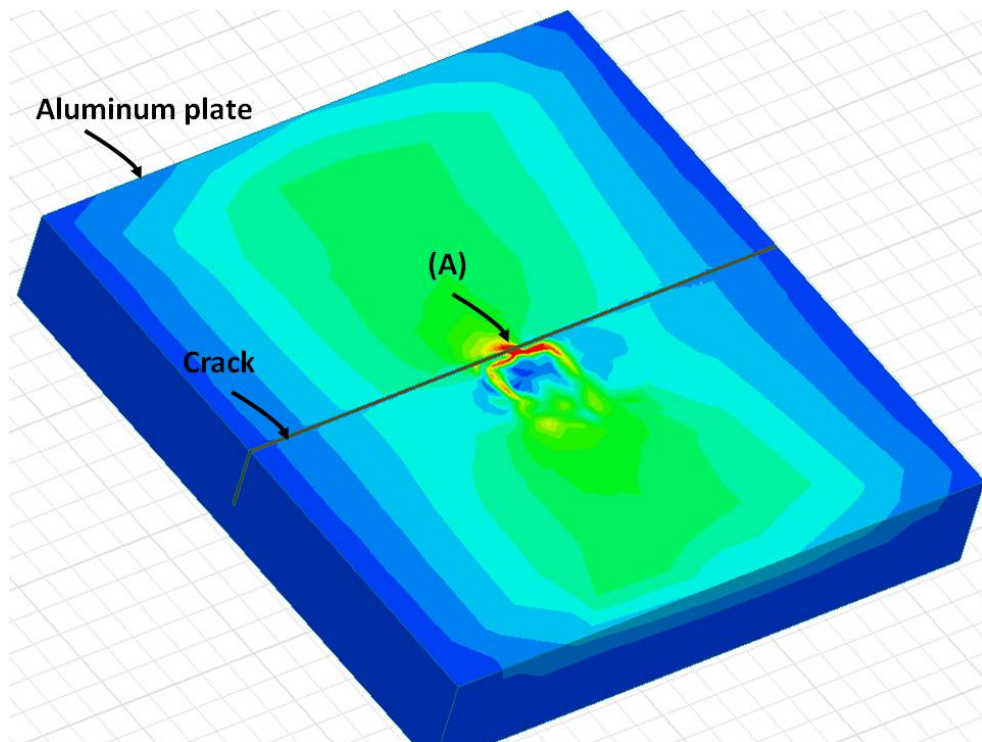


Figure 3.2: Current distribution on an aluminum plate for a crack with a width and depth of $100\mu\text{m}$ and 2mm , respectively.

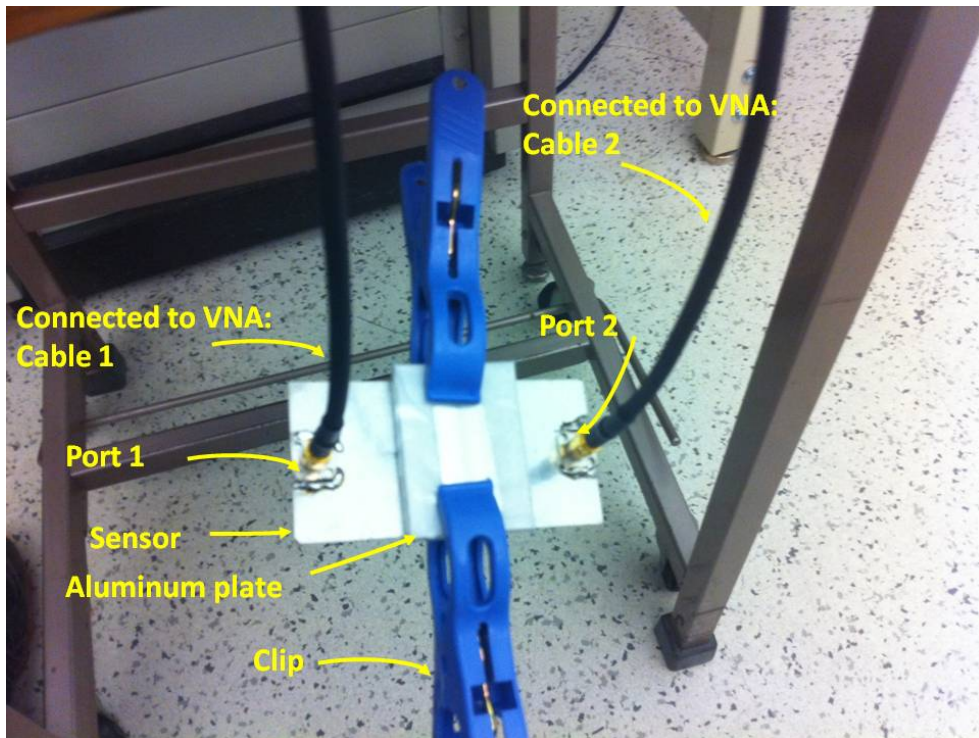


Figure 3.3: The experimental setup.

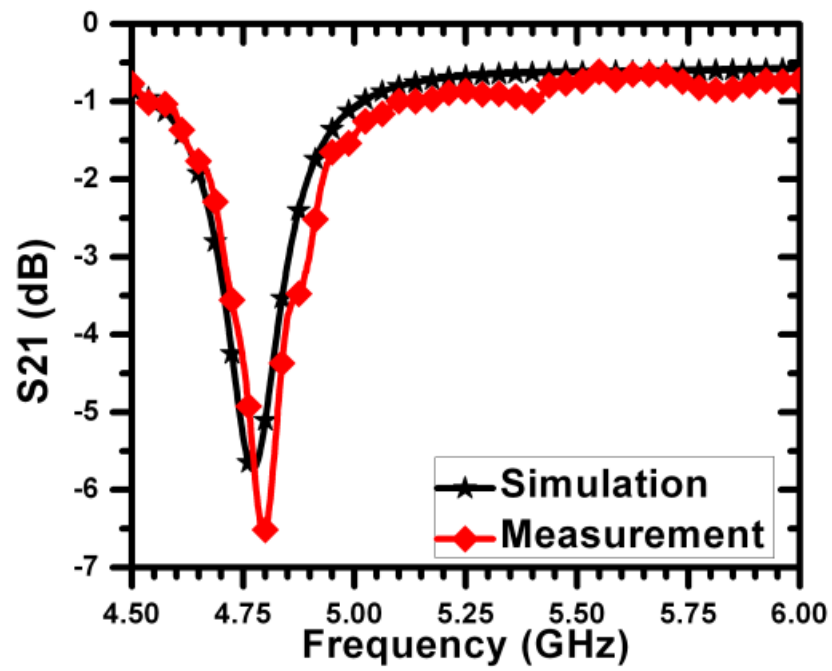


Figure 3.4: The frequency of minimum transmission for both simulated and experimental results in the case of a crack with a width and depth of $100\mu\text{m}$ and 2 mm , respectively.

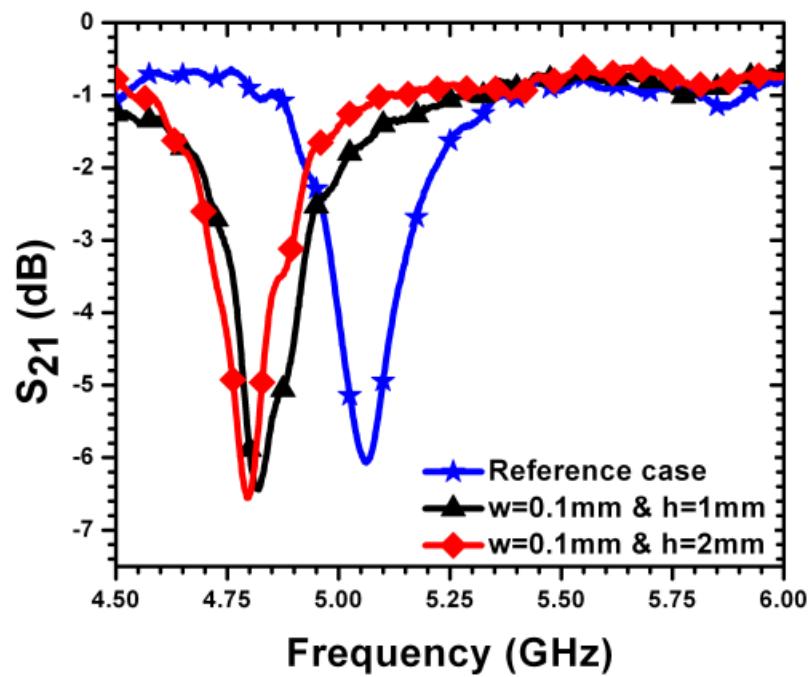


Figure 3.5: Minimum transmission of the sensor for a crack width (w) of $100\ \mu\text{m}$ compared with solid aluminium. For case 1, the crack depth (h) is 2 mm. For case 2, the crack depth (h) is 1 mm.

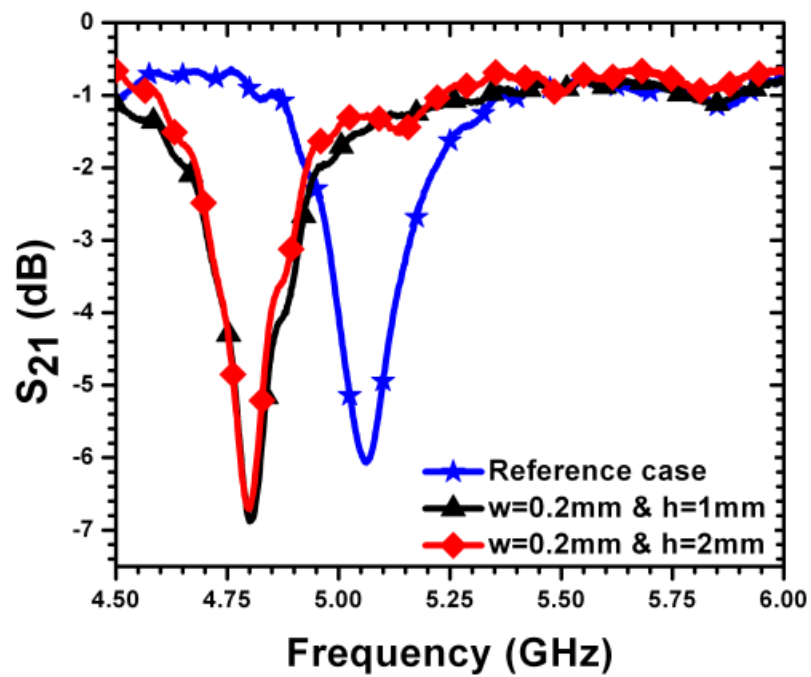


Figure 3.6: Minimum transmission of the sensor for a crack width (w) of $200\ \mu\text{m}$ compared with solid aluminium. For case 1, the crack depth (h) is 2 mm. For case 2, the crack depth (h) is 1 mm.

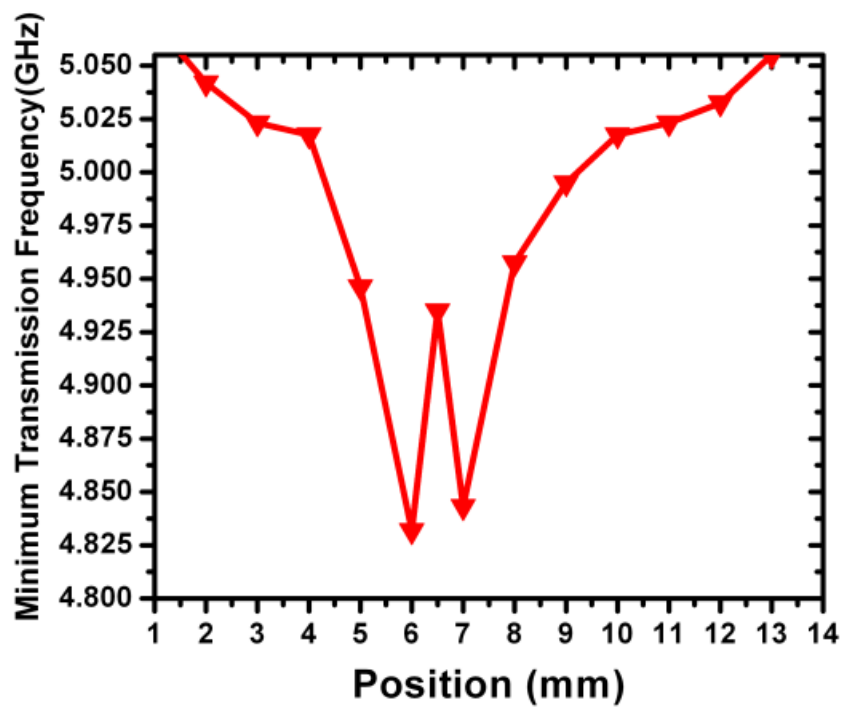


Figure 3.7: Shift in the minimum transmission frequency as a function of the position along a straight line that is perpendicular to the cracks.

Chapter 4

Sensitivity Enhancement of Crack Detection and Miniaturization of CSRR

4.1 Filling a Crack with a Dielectric Material

In this work, the proposed sensor was essentially intended to detect cracks having widths of $100\ \mu\text{m}$ and $200\ \mu\text{m}$, each with two different depths. However, one can investigate the limitations of this sensor for detecting smaller cracks. Due to milling machine limitations, fabricating a crack smaller than $100\ \mu\text{m}$ needs another technology. Interestingly, a smart way is considered to test the sensor's limitation by investigating the current distribution on the aluminum plate as shown in Fig. 3.2. According to the current distribution, charges are accumulated on the edges of the crack, and the capacitance is established. Hence, the resonance frequency of the CSRR exhibits a change. However, the equivalent circuit of the CSRR and integration with the crack are beyond the scope of this work and will be considered in future work. In general, the value of a capacitance depends proportionally on three critical factors: the area of the capacitance plates, the distance between the plates, and the dielectric constant of the material between the plates. For the aforementioned limitations, shrinking the width of a crack to smaller than $100\ \mu\text{m}$ was not possible. However, one can change the material filling a crack to a dielectric material. Hence, the capacitance increases proportionally. For demonstration purposes, a crack with a width of $200\ \mu\text{m}$ and a depth of 2mm was filled with silicone oil with a dielectric constant of 2.70. Figure 4.1 shows the frequency of the minimum transmission coefficient when the sensor is scanning the crack.

A shift of more than 435 MHz was registered with respect to the case of solid aluminum, without a crack. Clearly, the proposed sensor has shown its ability and sensitivity for crack detection, even ones smaller than $100 \mu\text{m}$. In addition, the research confirms the delectability of cracks is increased using silicon oil.

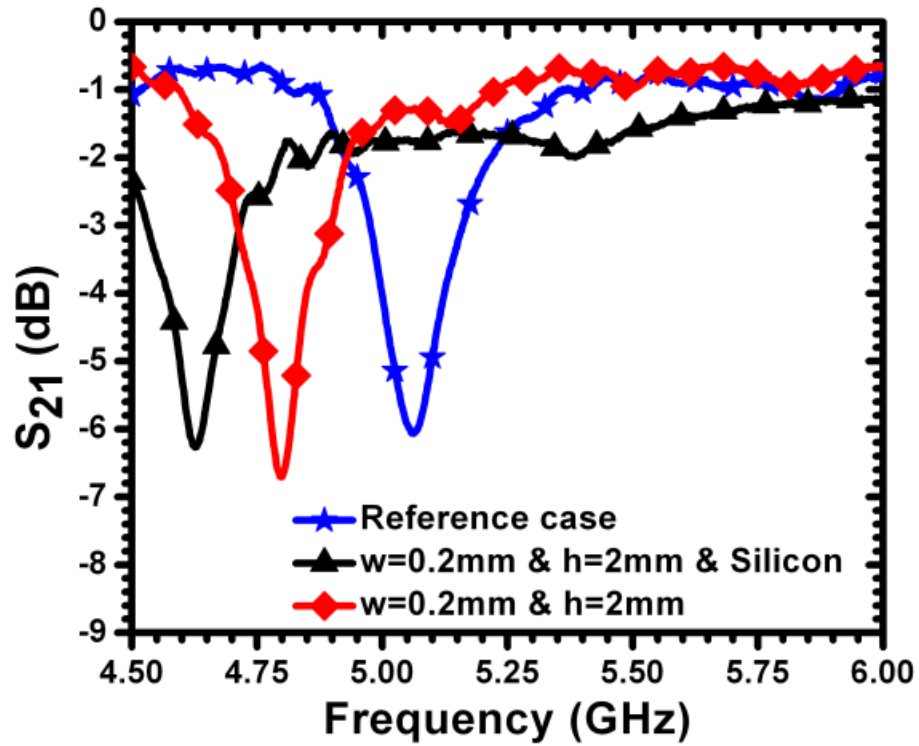


Figure 4.1: Minimum transmission of the sensor for a crack width (w) of $200 \mu\text{m}$ and depth of 2 mm: for case 1, a solid aluminum; case 2, the crack without silicon oil; case 3, the crack filled with silicon oil

4.2 Increasing the Total Inductance of CSRR for Miniaturizing Purposes

As shown in Fig. 2.4, at the resonance frequency of a CSRR, the current surface density is highly concentrated at the two narrow lines, which indicates that the magnetic field is confined around them. Therefore, one can investigate replacing these two narrow lines with two inductors, lumped-elements. For validation purposes, the full-wave simulation HFSS was used to simulate a CSRR by removing the two narrow lines (A and B) shown in Fig. 2.4 and adding two inductors with the same value of 20nH. The dimensions of the sensor were kept the same, except that the outer ring was changed to 6 mm. The minimum transmission coefficient of the sensor is shown in Fig. 4.2, and strong agreement between the measurement and simulation is observed. The experimental result of the CSRR, after adding the two inductors, shows a shift of more than 1.89 GHz, illustrated in Fig. 4.3. After adding the two inductors, the surface plane of the sensor is no longer smooth; consequently, one can use a reliable model designed in HFSS to validate the ability and sensitivity of the sensor in crack detection. The proposed idea of adding the two inductors was intended to enhance crack-detection ability. However, using lumped elements has the advantage of miniaturizing the CSRR, but the two inductors confine the magnetic field inside the inductors. As a result, the resonance frequency exhibited a very small shift after the sensor was passed over a crack (not shown). This result led moving to another direction. The idea of increasing the total inductance of the CSRR is kept for sensitivity enhancement purposes, but another novel idea to increase the inductance is used by implementing distributed elements instead of lumped elements.

Using distributed elements has the advantage of keeping the sensor surface smooth. Thus, the sensor can be passed over a crack easily. In addition, the sensor will be easy to fabricate using printed circuit board technology. From the current distribution shown in Fig. 2.4, region A, where the sensing element is observed, essentially contributes to construct the total inductance of the CSRR resonator at the resonance frequency. Interestingly, by increasing the length of the narrow line at region A, the current surface density is distributed at the resonance frequency as shown in Fig. 4.4. Consequently, the total inductance was increased so that the resonance frequency shifted an approximately 50% with respect to the original CSRR design responses, as shown at Fig. 4.5. Figure 4.6 shows that a 100 μm wide and 2 mm deep crack results in a frequency shift of more than 70 MHz. Obviously, increasing the total inductance of a CSRR for miniaturizing purposes using either lumped or distributed elements is verified. However, the sensitivity of the CSRR is decreased for crack detection, but the sensor works at low frequency.

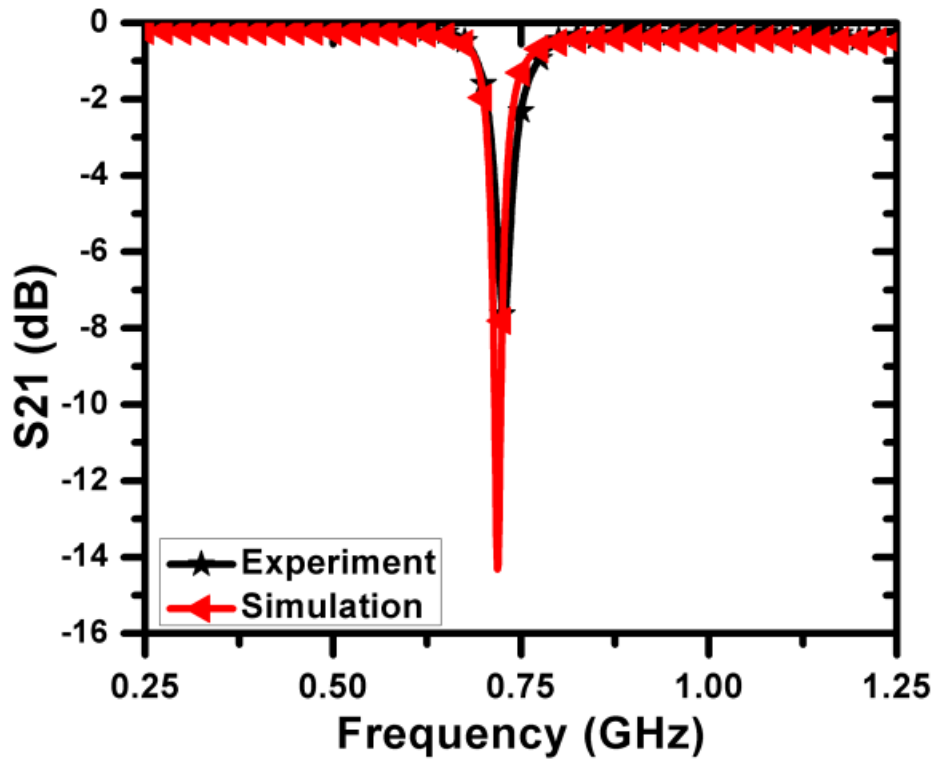


Figure 4.2: Minimum transmission coefficient of the sensor obtained from the full-wave simulator HFSS and measurement of 6 mm CSRR for the case without a crack after adding the two inductors of value 20 nH.

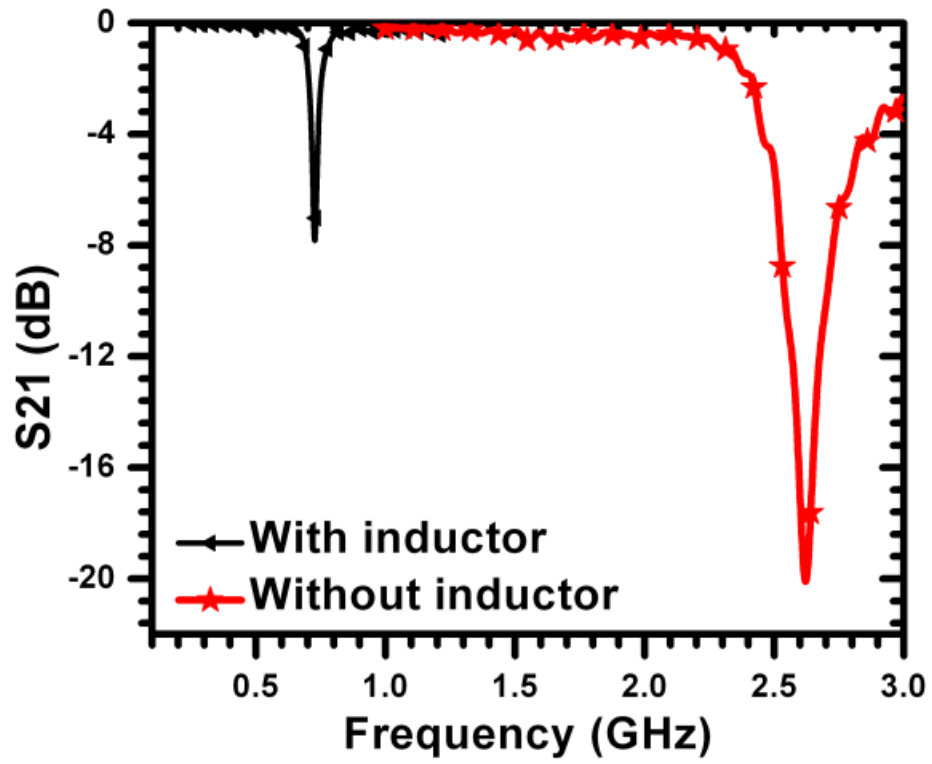


Figure 4.3: Minimum transmission coefficient of the sensor obtained from measurement with and without inductors of 6 mm CSRR.

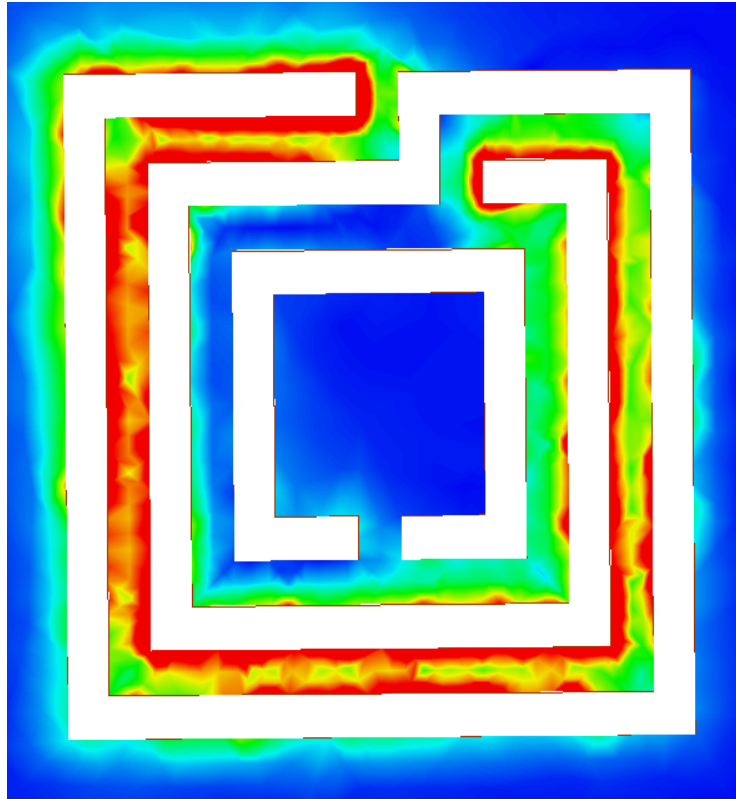


Figure 4.4: Simulated current distribution on a new design of CSRR sensor using spiral shape at the resonance frequency of around 3.781 GHz.

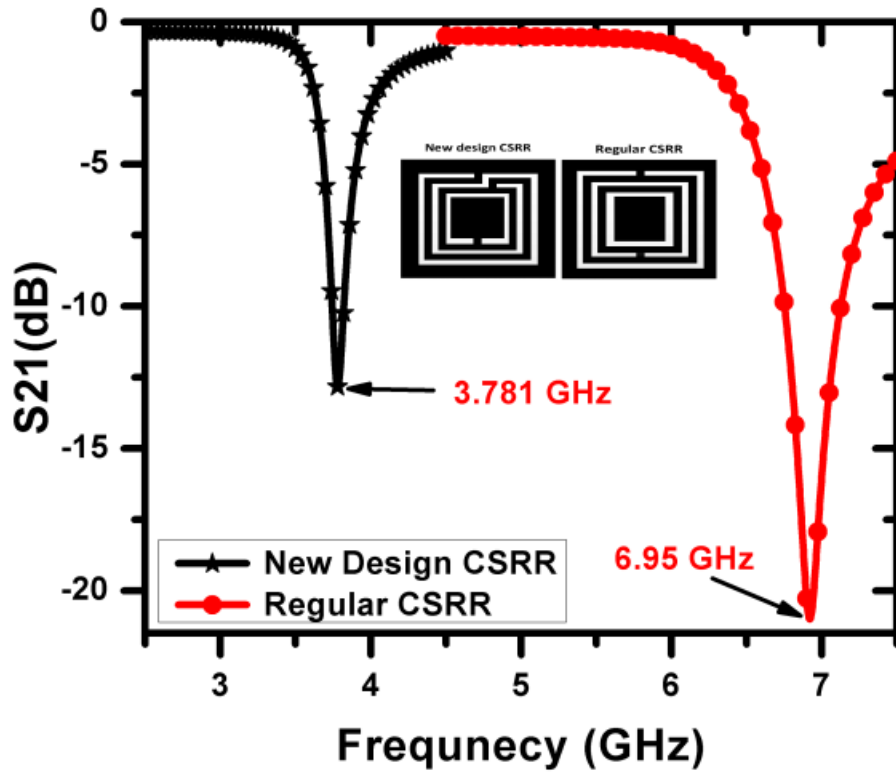


Figure 4.5: Minimum transmission coefficient of the two sensor obtained from the full-wave simulator HFSS at the resonance frequency of 3 mm CSRR.

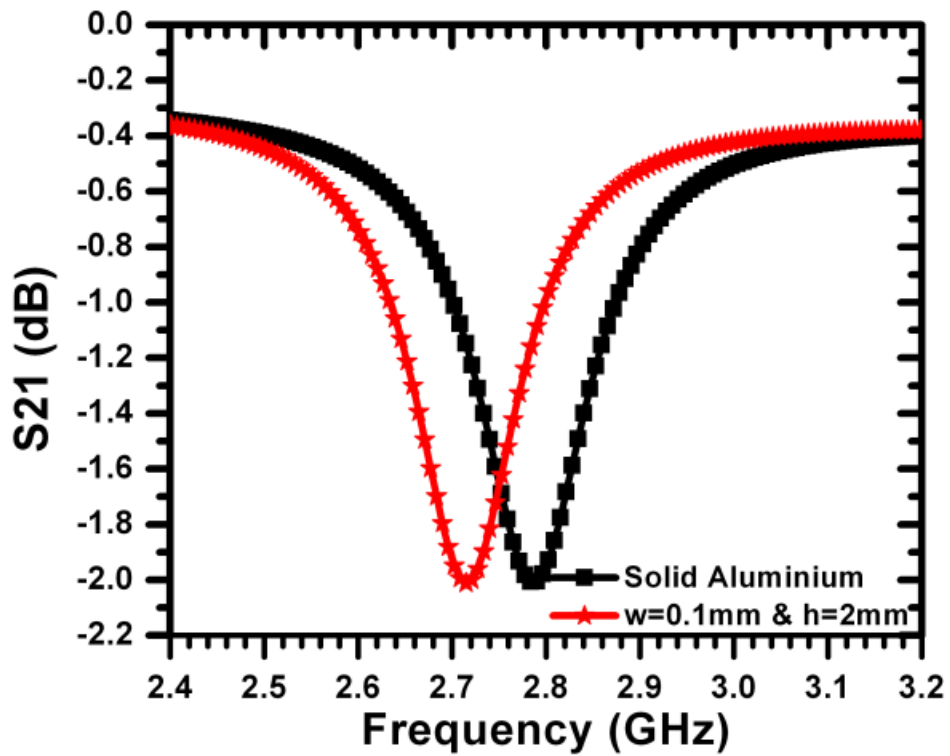


Figure 4.6: Minimum transmission of the new design of CSRR sensor using spiral shape for crack width (w) of $100 \mu\text{m}$ and the crack depth (h) is 2 mm compared with solid aluminium.

Chapter 5

Conclusion

5.1 Conclusion

This work has presented a new method for sub-millimeter crack detection on conductive surfaces. The principle of the sensor is numerically and experimentally verified. An electrically small resonator illuminated by a microstrip transmission line, a CSRR for this study, is used as a sensor to detect cracks in metallic surfaces covered by a dielectric layer. The sensing element in the CSRR is much smaller than the wavelength of the excitation source. The sensing mechanism is activated when the sensing element is placed underneath and in close proximity to a crack; the resonator (CSRR) is then loaded, so the minimum transmission coefficient (S_{21}) at the resonance frequency shifts. The dielectric material, teflon film, between sensing the sensing element in the CSRR and the crack, and the metallic properties of the cracked material will determine the total shift in the resonance frequency.

The simulations and measurements were carried out on aluminum plates. The sensor operates at 6.95 GHz and exhibits a more than 240 MHz resonance frequency shift for a crack width of 100 μm . A shift of more than 435 MHz was observed in the case of a solid aluminum plate with a 200 μm crack filled with silicon oil. For miniaturizing purposes, the total inductance of a CSRR was increased using either lumped or distributed elements. The designs has been numerically verified. The resonance frequency shifted by an approximately 50% with respect to the original CSRR design responses. In addition, a frequency shift of more than 70 MHz occurred when a crack a 100 μm wide and 2 mm deep was scanned by the sensor. Compared to the other microwave methods presented in the literature, the sensor operates at a lower frequency, has significantly higher sensitivity, and is relatively very inexpensive.

References

- [1] Ansys HFSS Version 13.0. ANSYS CORPORATION. <http://www.ansys.com>.
- [2] M.A. Abou-Khousa, S. Kharkovsky, and R. Zoughi. Novel near-field millimeter-wave differential probe using a loaded modulated aperture. *Instrumentation and Measurement, IEEE Transactions on*, 58(5):1273–1282, may 2009.
- [3] S.M. Anlage, V.V. Talanov, and A.R. Schwartz. Principles of near-field microwave microscopy. *Scanning Probe Microscopy: Electrical and Electromechanical Phenomena at the Nanoscale*, 1:215–253, 2007.
- [4] EA Ash and G. Nicholls. Super-resolution aperture scanning microscope. 1972.
- [5] J. Bannantine. Fundamentals of metal fatigue analysis. *Prentice Hall, 1990*, page 273, 1990.
- [6] T. Chady, M. Enokizono, and R. Sikora. Crack detection and recognition using an eddy current differential probe. *Magnetics, IEEE Transactions on*, 35(3):1849–1852, 1999.
- [7] U. Durig, DW Pohl, and F. Rohner. Near-field optical-scanning microscopy. *Journal of applied physics*, 59(10):3318–3327, 1986.
- [8] F. Falcone, T. Lopetegi, M. A. G. Laso, J. D. Baena, J. Bonache, M. Beruete, R. Marqués, F. Martín, and M. Sorolla. Babinet principle applied to the design of metasurfaces and metamaterials. 93(19):197401, Nov 2004.
- [9] W.C. Fitzgerald, M.N. Davis, J.L. Blackshire, J.F. Maguire, and D.B. Mast. Evanescent microwave sensor scanning for detection of sub-coating corrosion. *Journal of Corrosion Science & Engineering*, 3:2000–2002, 2002.

- [10] C. Huber, H. Abiri, S. Ganchev, and R. Zoughi. Modeling of surface hairline-crack detection in metals under coatings using an open-ended rectangular waveguide. *Microwave Theory and Techniques, IEEE Transactions on*, 45(11):2049–2057, nov 1997.
- [11] C. Huber, H. Abiri, S.I. Ganchev, and R. Zoughi. Analysis of the ‘crack characteristic signal’ using a generalized scattering matrix representation. *Microwave Theory and Techniques, IEEE Transactions on*, 45(4):477–484, apr 1997.
- [12] C. Huber, S. Ganchev, R. Mirshahi, J. Easter, and R. Zoughi. Remote detection of surface cracks/ slots using open-ended rectangular waveguide sensors. *Nondestructive Testing and Evaluation*, 13(4):227–237, 1997.
- [13] J. Kerouedan, P. Qufflec, P. Talbot, C. Quendo, S. Blasi, and A. Brun. Detection of micro-cracks on metal surfaces using near-field microwave dual-behavior resonator filters. *Measurement Science and Technology*, 19(10):105701, 2008.
- [14] S. Kharkovsky, M.T. Ghasr, and R. Zoughi. Near-field millimeter-wave imaging of exposed and covered fatigue cracks. *Instrumentation and Measurement, IEEE Transactions on*, 58(7):2367–2370, july 2009.
- [15] H.J. Lee, H.S. Lee, K.H. Yoo, and J.G. Yook. Dna sensing using split-ring resonator alone at microwave regime. *Journal of Applied Physics*, 108(1):014908–014908, 2010.
- [16] F. Mazlumi, S. Sadeghi, and R. Moini. Interaction of rectangular open-ended waveguide with surface tilted long cracks in metals. *Instrumentation and Measurement, IEEE Transactions on*, 55(6):2191–2197, Dec. 2006.
- [17] F. Mazlumi, S.H.H. Sadeghi, and R. Moini. Using open-ended rectangular waveguide probe for detection and sizing of fatigue cracks in metals. *Electronics Letters*, 41(6):334–335, march 2005.
- [18] A. McClanahan, S. Kharkovsky, A.R. Maxon, R. Zoughi, and D.D. Palmer. Depth evaluation of shallow surface cracks in metals using rectangular waveguides at millimeter-wave frequencies. *Instrumentation and Measurement, IEEE Transactions on*, 59(6):1693–1704, june 2010.
- [19] Irshad Mohammad and Haiying Huang. An antenna sensor for crack detection and monitoring. *ADVANCES IN STRUCTURAL ENGINEERING*, 14(1):47–53, FEB 2011.

- [20] H.H. Park, Y.H. Cho, and H.J. Eom. Surface crack detection using flanged parallel-plate waveguide. *Electronics Letters*, 37(25):1526–1527, dec 2001.
- [21] J.B. Pendry, A.J. Holden, D.J. Robbins, and W.J. Stewart. Magnetism from conductors and enhanced nonlinear phenomena. 47(11):2075–2084, Nov 1999.
- [22] M. Puentes, C. Weiss, M. Schussler, and R. Jakoby. Sensor array based on split ring resonators for analysis of organic tissues. In *Microwave Symposium Digest (MTT), 2011 IEEE MTT-S International*, pages 1–4. IEEE, 2011.
- [23] N. Qaddoumi, E. Ranu, JD McColskey, R. Mirshahi, and R. Zoughi. Microwave detection of stress-induced fatigue cracks in steel and potential for crack opening determination. *Journal of Research in Nondestructive Evaluation*, 12(2):87–103, 2000.
- [24] Chin-Yung Yeh and Reza Zoughi. A novel microwave method for detection of long surface cracks in metals. *Instrumentation and Measurement, IEEE Transactions on*, 43(5):719–725, oct 1994.
- [25] R. Zoughi, S.I. Ganchev, and C. Huber. Measurement parameter optimization for surface crack detection in metals using an open-ended waveguide probe. In *Instrumentation and Measurement Technology Conference, 1996. IMTC-96. Conference Proceedings. 'Quality Measurements: The Indispensable Bridge between Theory and Reality'*, IEEE, volume 2, pages 1391–1394 vol.2, 1996.
- [26] R. Zoughi and S. Kharkovsky. Microwave and millimetre wave sensors for crack detection. *Fatigue & Fracture of Engineering Materials & Structures*, 31(8):695–713, 2008.